Electron-nucleus interactions in few-electron Fe ions

W. R. Phillips, J. Copnell, and D. W. Banes
University of Manchester, Manchester M13 9PL, United Kingdom

K. E. Rehm, I. Ahmad, B. G. Glagola, W. Henning, W. Kutschera, and J. P. Schiffer
Physics Division, Argonne National Laboratory, Argonne, Illinois 60439

(Received 25 September 1992)

Measurements have been made of the total decay rates of the 14.4-keV level in the ^{57}Fe nucleus in highly charged Fe ions having one to six electrons outside the nucleus. Results are 10.0(9), 7.06(18), 7.36(14), 7.16(11), 7.10(23), 7.28(25), and 6.92(46), in units of 10^6 s^{-1}, for ions of charge states q from 25 to 19, respectively. For the $q=25$ single-electron ion the result quoted is for the ion in which the spin of the $1s_{1/2}$ electron and the excited nuclear state are coupled to give quantum number $F=1$. Measurements have also been made of the K-shell fluorescent yields for ions in charge states q (before K-vacancy production) from 22 to 19. Results are 0.62(1), 0.50(1), 0.48(2), and 0.50(6), respectively. These data are discussed and compared with theoretical predictions.

PACS number(s): 35.10.−d, 35.80.+s, 32.80.Hd, 23.20.Nx

I. INTRODUCTION

It is well known that nuclear decays can be influenced by changes in the atomic environment. However, very few detailed measurements of these effects in highly charged atoms have been performed. Data on highly charged ions are of interest and importance in many fields of science. Plasma studies offer several examples: transitions in Fe XVII to Fe XXIV have been used [1,2] to determine electron densities and temperatures in solar flares, and lines in He-like Fe ions have been observed [3] and used for diagnostic purposes in hot laboratory plasmas. Dielectronic recombination (DER) [4] can influence the lifetimes of heavy-ion beams in electron-cooled storage rings. The first stage of the DER process is the inverse of the Auger effect, and cross sections for DER in ions of a given charge are related to fluorescent yields in excited ions with charge decreased by one unit. From the theoretical point of view measurements of the electronic properties of highly charged ions provide new and simple opportunities for testing the ability of relativistic mean-field theories [5] to treat electron correlations.

The absence of outer electrons in highly charged ions modifies the wave functions of the remaining electrons and hence their influence on nuclear decays. This effect is utilized in our experiments, where internal conversion coefficients (ICC's) and K-shell fluorescent yields have been measured in different ionic charge states, q. Preliminary results of the work have been published previously [6,7]. A technique was developed for the experiments and applied to measurements on ^{57}Fe ions. The ^{57}Fe nucleus has a first excited state at 14.4 keV with a half-life of 98.1(3) ns in the neutral atom [8]. This level decays predominantly by a magnetic dipole ($M1$) transition which is highly converted. The total ICC, α_T, has been measured [8] to be 8.18(11) and the predicted [9] ratio of the K-shell to L-shell conversion is 9.79. In our experiments the charge change following IC decay of the 14.4-keV level during passage of a ^{57}Fe beam through a magnetic spectrograph was used to measure the IC rates and K-shell fluorescent yields as a function of ionic charge state.

There have been several previous observations of the influence of outer electrons on IC decay rates. In ^{57}Fe, for example, these chemical effects [9] can change α_T by up to 6×10^{-4}. The influence of changing inner-shell electron numbers on IC has been investigated in a few cases. Experiments [10] on ^{197}Au involved the removal of too few electrons for effects to be observable; experiments [11] on transitions in ^{18}F showed that K-conversion coefficients were reduced in rapidly recoiling ^{18}F nuclei in a mixture of highly charged ions. The present experiments make IC measurements on identified, highly charged ions.

Section II describes the principles and details of the experimental method. Section III describes the analysis procedures used, and Sec. IV discusses the results and compares them with theoretical predictions.

II. EXPERIMENT

Several short-lived excited states in the ^{57}Fe nucleus, above the 14.4-keV level, are connected to the ground state by large electric-quadrupole ($E2$) matrix elements and also deexcite with large branching to the 14.4-keV level. A significant population of the first excited state in a beam of ^{57}Fe scattered from a Au target can thus be produced by multiple Coulomb excitation. A very short time ($\leq10^{-10}$ s) after leaving the target, ^{57}Fe ions in a secondary beam selected at a suitable angle of scattering will settle into a mix of charge states centered on a mean charge q, with each charge state q being comprised of a mix of long-lived electronic states. If no charge-changing events could occur, passage of such a secondary beam through a magnetic spectrograph would result in a simple pattern of events in the focal plane of the instrument.

This pattern would consist of separate peaks at positions corresponding to the different magnetic rigidities of the several charge states, the number of counts in the peaks giving the distribution of ions among the charge states. There would be essentially no counts in between the peaks. Collisions between ions and residual gas in the spectrograph are very rare; the measured probability of a charge-changing event occurring due to collisions with the residual gas was less than one in 10^5 for a ^{58}Ni beam of energy 300 MeV. However, in the case of a secondary beam of ^{57}Fe, charge changing can occur within the spectrometer as a result of IC decays of the 14.4-keV level. These produce events in the focal plane lying between the peaks corresponding to no change in charge, with positions which depend on where the change of charge took place and by how much the charge changed. Observation of these events gives information on the IC rates and fluorescent yields as a function of initial charge q.

Gold targets of thickness about 100 $\mu g\,cm^{-2}$ were bombarded with beams of ^{57}Fe at an energy of 346 MeV. The beams were provided by the ATLAS accelerator at the Argonne National Laboratory. Ions scattered at laboratory angles θ_L were accepted in an Enge [12] split-pole spectrograph through a rectangular aperture subtending a solid angle of 0.25 msr and an angular width $\Delta\theta_L = 0.36°$ at the target. For θ_L near 40°, ions entered the spectrograph about 18 ns after leaving the target and in a distribution of charge states centered around $\bar{q} \approx 22.5$.

After the secondary beam enters the magnetic field, IC decays of the 14.4-keV level may change the charge state by $\Delta q = +1$ or $+2$ depending on whether a K vacancy generated by the nuclear decay is filled with the emission of a K x-ray or an Auger electron. After emerging from the magnetic field of the spectrograph, the ions were detected in the focal plane with a position-sensitive gas detector [13], which measured total energy and nuclear charge of the incoming ion, position in the focal plane, and time of flight from target to focal plane. These data were used to construct two-dimensional spectra of both energy versus position and time of flight versus position. Windows were placed on these two-dimensional spectra requiring that events, within narrow ranges, had the correct energy and time of flight for a given position in the focal plane. This produced one-dimensional spectra giving the position distribution of ^{57}Fe ions along the focal plane.

Preliminary runs were made to determine the best laboratory angle for accumulating data. The absolute yield of the 14.4-keV level, as determined from the number of charge-changed events, increases with decreasing θ_L. However, the ratio of the charge-changed to -unchanged events decreases as the scattering angle moves forward because the elastic-scattering cross section increases faster than the inelastic. The scattering angle of 40° represents the best compromise between absolute yield of the 14.4-keV level and uncertainties caused by large numbers of events in the unchanged-charge peaks.

Long runs were made at $\theta_L = 40°$, separated by runs at 50°, 55°, 60° and 65° made in order to study the possible influence of transfer reactions. Figure 1 shows a position spectrum obtained from a short run at 10.0°, where the scattered ^{57}Fe ions have only a very small fraction of nuclei in the excited state. The relatively few events observed between the large unchanged charge peaks are estimated to arise mainly from decays of the 14.4-keV level. Figure 2(a) shows a position spectrum obtained at 40°.

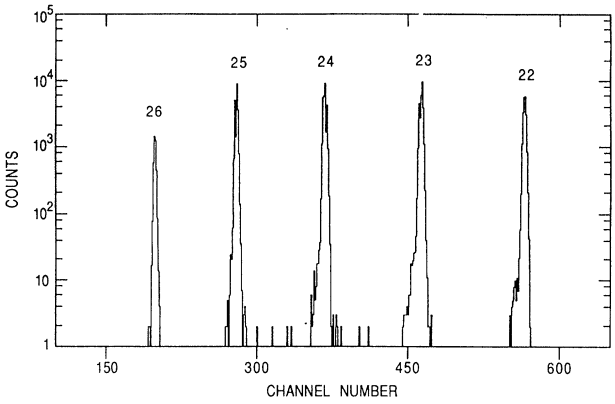

FIG. 1. Position spectrum obtained at $\theta_L = 10°$ with the spectrometer set to observe charge states with $q = 22$–26. The peaks in the figure correspond to $q = 22$–26, $\Delta q = 0$.

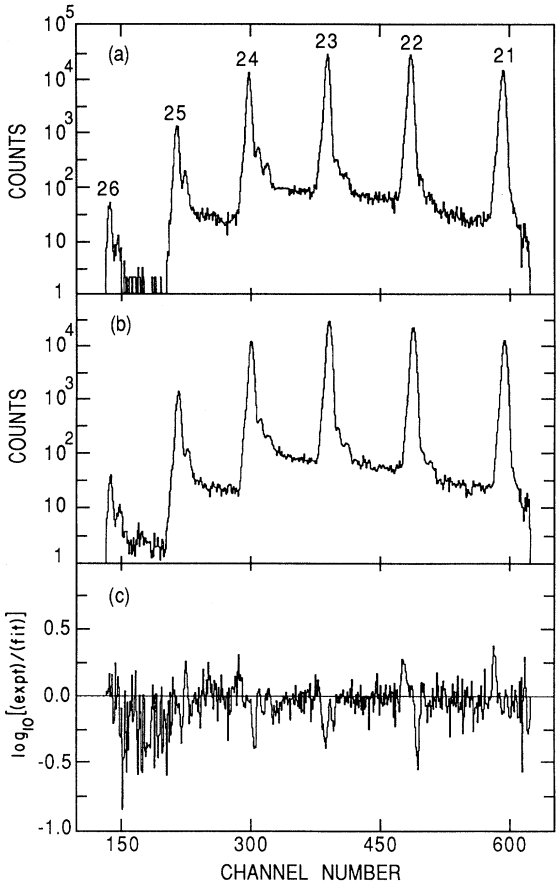

FIG. 2. (a) Position spectrum obtained at $\theta_L = 40°$ with the spectrometer set to observe charge states with $q = 21$–26. (b) Corresponding Monte Carlo best-fit spectrum. (c) Ratio of spectra a and b: $\log_{10}$ [(experiment)/(Monte Carlo)].

Between the main peaks lie the events corresponding to $\Delta q = +1$ or $+2$ processes brought about by IC decays in the magnet. Near the main peaks are small subsidiary peaks which arise from charge changes in the gap between the two poles of the split-pole spectrograph. The magnetic field in this gap is small, and a charge change $\Delta q = +1$ anywhere in the gap from an initial charge state $(q-1)$ results in events at approximately the same place in the focal plane, producing the subsidiary peak nearest to the main peak from unchanged charge state q. The second subsidiary peak, where appropriate, comes from $\Delta q = +2$ ions with initial charge $(q-2)$. There is only one subsidiary peak near the $q=25$ and 26 unchanged charge peak because ions initially in charge states $q=23$ and 24 can only undergo changes $\Delta q = +1$, as discussed in Sec. IV.

III. ANALYSIS

A. General considerations

The analysis of spectra like the one shown in Fig. 2(a) was effected by performing a Monte Carlo simulation of the trajectories of ions through the spectrometer using decay constants and fluorescent yields for different charge states as input parameters. These determinations of the histories of ensembles of ions leaving the target were made using the ion-optical code RAYTRACE [14], modified to include charge changes $\Delta q = +1$ and $+2$ along their trajectories. The parameters of the simulation were obtained by χ^2 minimization to the observed patterns of events in the focal plane. These parameters are considered in the following simplified description of the physical processes occurring in the scattered ion beam after leaving the target.

Less than 10^{-10} s after leaving the target, autoionizing processes have ceased and the number of ^{57}Fe ions in charge state q is N_q^0. The fraction of nuclei in the 14.4-keV level is assumed to be independent of charge state and equal to f^0. All ions take a time of t_1 (~ 18 ns) to reach the magnet entrance, at which time the number of ions in charge state q is N_q^1 and the fraction of nuclei in the 14.4-keV state is f_q^1 depending now on q. N_q^1 is equal to N_q^0 less the number that have changed charge due to IC decays on the way to the magnet entrance plus the number that had lower charge states $(q-1, q-2)$ before but changed to charge state q after IC decay:

$$\begin{aligned} N_q^1 = N_q^0 &- f^0 N_q^0 R_q(\rho_{q,q+1}+\rho_{q,q+2}) \\ &+ f^0 N_{q-1}^0 R_{q-1}\rho_{q-1,q} \\ &+ f^0 N_{q-2}^0 R_{q-2}\rho_{q-2,q} \ . \end{aligned} \tag{1}$$

In this formula

$$R_q = 1-\exp(-\lambda_q t_1) \ , \tag{2}$$

is the number of nuclei that decayed within the time t_1,

$$\rho_{q,q+1} = \frac{\lambda_{\mathrm{IC}\,q}}{\lambda_q}\omega_q \tag{3}$$

and

$$\rho_{q,q+2} = \frac{\lambda_{\mathrm{IC}\,q}}{\lambda_q}(1-\omega_q) \ , \tag{4}$$

are the fractions of decays that result in an increase of the charge state by one or two units, respectively, and

$$\lambda_q = \lambda_{\mathrm{IC}\,q} + \lambda_\gamma \ . \tag{5}$$

λ_q is the total decay probability per unit time of the 14.4-keV level in charge state q, averaged over the electronic states in existence in those ions from the time of leaving the target to time t_1. $\lambda_{\mathrm{IC}\,q}$ is the IC decay rate in charge state q, and ω_q is the fraction of IC decays in which a K hole is filled by photon emission. λ_γ is the γ-ray decay rate of the 14.4-keV level. We now have

$$f_q^1 = f^0 N_q^0 / N_q^1 \exp(-\lambda_q t_1) \ . \tag{6}$$

The above equations describe the ion-beam conditions on entry to the spectrograph. Within the spectrograph, an ion's trajectory is determined by its charge and modified by any charge change depending on the location of the change and on the value of the new charge state ($\Delta q = +1$ or $+2$). For ions in charge state q, the number of $\Delta q = +1$ events in the interval t to $(t+dt)$ is given by

$$dN_q(t, \Delta_q = +1) = -\lambda_q f_q^t N_q^t \exp(-\lambda_q t)\rho_{q,q+1} dt \ . \tag{7}$$

These events produce ions with positions in the focal plane dependent upon t and lying between unchanged charge peaks q and $(q+1)$. The number of $\Delta q = +2$ events from ions in charge state q in the interval t to $(t+dt)$ is given by

$$dN_q(t, \Delta_q = +2) = -\lambda_q f_q^t N_q^t \exp(-\lambda_q t)\rho_{q,q+2} dt \ . \tag{8}$$

[A $\Delta q = +2$ event from charge state $(q-1)$ occurring late in an ion's trajectory can place the event at the same position in the focal plane as a $\Delta q = +1$ event occurring early in the trajectory.] The above set of equations was used to simulate the experiments and predict patterns of events in the focal plane for different values of input parameters.

B. Dependence on the atomic spin

The description given above is oversimplified and must be modified for the $q=25$ ions studied in these experiments, where the single electron is in the $1s_{1/2}$ orbit (see Sec. IV A). Those $q=25$ ions which have the nucleus in the $\frac{3}{2}^-$, 14.4-keV excited state have values of the total angular momentum quantum number F equal to 1 or 2. Due to the small density near the nucleus of d-state continuum electrons, these contribute only weakly [15] to the $M1$ IC process, which proceeds almost entirely with production of $s_{1/2}$ continuum electrons. The d-state contribution to the $q=25$ IC is calculated to be less than 1.2% of that of the s state. Hence to a good approximation the $F=2$ ions cannot decay by IC to the bare $\frac{1}{2}^-$ nuclear ground state. The $q=25$ ions were thus treated as a statistical mix of the two components with different F values, a fraction $\frac{5}{8}$ of N_{25}^0 having a total decay probability $\lambda_{25}(F=2)$ equal to the γ decay rate λ_γ, and a fraction $\frac{3}{8}$ having a total decay probability $\lambda_{25}(F=1)$ equal to the

sum of λ_γ and $\lambda_{IC,25}(F=1)$. In principle, the $q=23$ ions studied, which have the configuration $(1s)^2(2s)^1\,^2S_{1/2}$ (see Sec. IV A) should be treated in the same way. However, the contribution of the electron in the $2s_{1/2}$ orbit to the IC decay is small and little error was made in using a single parameter $\lambda_{23}=(\lambda_\gamma+\lambda_{IC,23})$ in the simulations. The parameter ω_{23} was set to unity, since Li-like Fe XXIV ions, after a few ns, have only one electron in the outer shells, and Auger emission after K-vacancy production is not possible.

C. Fitting procedure

The parameter f^0 was not varied; it was determined directly from the counts in the position spectra. The total number of decays within the magnet in which ions with initial charge q increase their charge is given by

$$\begin{aligned}\Delta N_q &= f_q^1 N_q^1[1-\exp(-\lambda_q \Delta t_q)](\rho_{q,q+1}+\rho_{q,q+2}) \\ &= f^0 N_q^0 \exp(-\lambda_q t_1)[1-\exp(-\lambda_q \Delta t_q)] \\ &\quad \times(\rho_{q,q+1}+\rho_{q,q+2}) ,\end{aligned} \tag{9}$$

using Eq. (6). The data are dominated by $q=21$, 22 and 23, for which RAYTRACE calculations give values of Δt_q, the time ions which do not change charge spend in the spectrograph, equal to 65, 62, and 59 ns, respectively. From the total number of charge-changed events obtained from the spectra, using $\Delta t_q=62$ ns and the neutral-atom values for all λ_q and $(\rho_{q,q=1}+\rho_{q,q+2})$ [7.07×10^6 s^{-1} and 0.9, respectively], f^0 can be determined with little procedural error. The values of f^0 extracted from two runs at 40° were 0.250(3) and 0.249(3), where the errors quoted are statistical. A value of $f^0=0.25$ was used in the simulations. We finally have the appropriate λ_q, N_q^0 and ρ_q as the set of input parameters which were varied to produce the best fits.

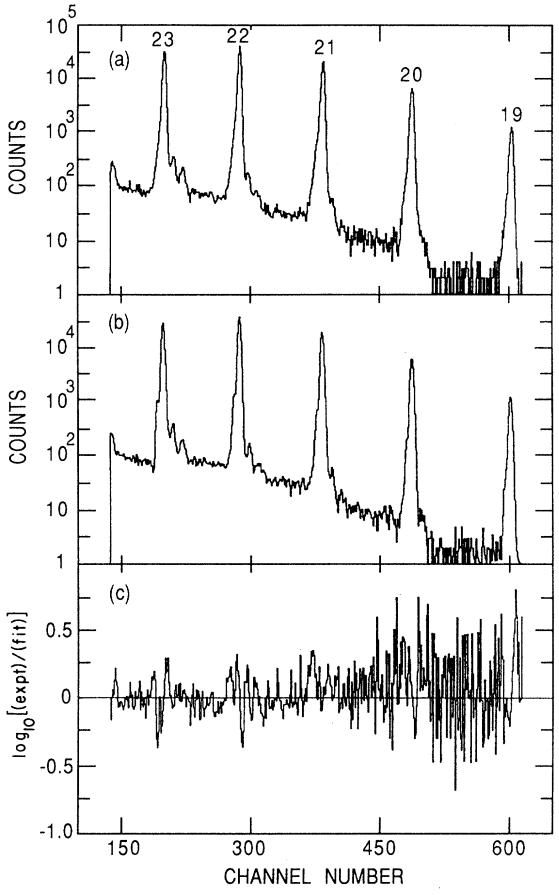

FIG. 3. (a) Position spectrum obtained at $\theta_L=40°$ with the spectrometer set to observe $q=19$–23 charge peaks. (b) Corresponding Monte Carlo best fit spectrum. (c) Ratio of spectra a and b: $\log_{10}$[(experiment)/(Monte Carlo)].

TABLE I. Values of transition probabilities λ_q and parameters ω_q obtained from fits to the experimental spectra together with deduced values of total conversion coefficients $\alpha_{IC\,q}$ and K-shell fluorescent yields ω_{Kq}. Errors given for λ_q and ω_q are a combination of statistical errors deduced from the distribution of the statistic χ^2 as a function of the several parameters, and uncertainties arising from the small spreads in parameter values obtained from different sets of simulations. The contributions from the latter source were at the 1% level for all charge states.

Initial charge	λ_q (10^6 s^{-1})	$\alpha_{IC\,q}$[a]	ω_q	ω_{Kq}[b]
25 ($F=1$)	10.0(9)	12.0(12)		
24	7.06(18)	8.17(33)		
23	7.36(14)	8.57(31)		
22	7.16(11)	8.30(28)	0.57(1)	0.62(1)
21	7.10(23)	8.22(38)	0.46(1)	0.50(1)
20	7.28(25)	8.45(41)	0.44(2)	0.48(2)
19	6.92(46)	7.99(64)	0.45(5)	0.50(6)

[a] $\alpha_{IC\,q}=(\lambda_q-\lambda_\gamma)/\lambda_\gamma$, with $\lambda_\gamma=7.7(2)\times10^5$ s^{-1} as calculated using lifetime and conversion-coefficient data [8] for the neutral atom.

[b] $\omega_{Kq}=\omega_q\lambda_{IC\,q}/\lambda_{Kq}$, with $\lambda_{IC\,q}/\lambda_{Kq}$ calculated as in Sec. IV B.

Figure 2(b) shows the best fit to the data of Fig. 2(a) as obtained from a χ^2 minimization. Figure 2(c) shows the difference between the best-fit simulation, Fig. 2(b), and the data of Fig. 2(a). Two runs at 40° with the spectrometer set to observe $q=21-26$ charge peaks were analyzed separately, as was a third run at 40° with the spectrometer set to observe $q=19-23$ charge peaks. The combined results are given in Table I. Figures 3(a)–3(c) show experimental and simulation data for the third run at 40°.

D. Influence of other effects (higher excited states, transfer reactions)

Before discussing these results, it is necessary to consider some effects neglected in the above analysis. On exit from the foil some of the nuclei in the ^{57}Fe ions are in the 136.5-keV excited state. This state has [8] a half-life of 8.69(25) ns and decays predominantly via photon emission to the 14.4-keV level. The lifetime of the 136.5-keV state in different charge states is thus approximately constant. If this state is populated significantly on exit from the target, the analysis routines discussed above would have to be modified, and would have to include a further parameter which gave the fraction of nuclei in the 136.5-keV level. At 346-MeV incident energy several nuclear states are initially populated by multiple Coulomb excitation processes. γ-ray branches downwards from these states, ending on the 136.5- and 14.4-keV levels, chiefly determine the relative population of the latter two nuclear levels immediately after foil exit. The information on higher-lying states needed to reliably estimate the relative population is not known. However, calculations which included the first five negative-parity states of the ^{57}Fe nucleus and which used reasonable couplings between the levels, and known γ-ray deexcitation branching ratios, suggest that the exit population of the 136.5-keV state was less than 20% of the nuclear excitations. Neglect of this population should have only a small influence on the results for λ_q due to the short lifetime of the 136.5-keV level, and smaller influence on the ω_q, since these depend only on the atomic configurations.

Another question is whether all of the events observed at 40° are ^{57}Fe ions. In order to estimate the fraction of processed events due to quasielastic nucleon transfer reactions, runs were taken at 50°, 55°, 60° and 65° near the grazing angle for nuclear collisions. At these angles one- and two-nucleon transfer reactions were observed. The cross sections extrapolated forward to 40° show that the fraction of quasielastic transfer events accepted in the narrow windows and thus recorded as ^{57}Fe ions was less than one percent.

An additional question arises about the use of the same average parameters λ_q and ω_q to describe decays in charge state q over the whole time from just after leaving the target to leaving the magnetic field of the spectrograph, about 80 ns later. This procedure would involve no ambiguity if the same mix of electron states prevailed in a given charge state over that time. This is very nearly true for $q=25$, 24, and 23 ions, less so for the others. The electron-state mixes, which determine the atomic properties the experiments are measuring, are discussed in the next section.

IV. DISCUSSION

A. *K*-shell fluorescent yields

The electron levels occupied in the charge states were determined by reference to existing data and to theoretical calculations of lifetimes made using the relativistic mean-field code GRASP [16]. Lifetimes for decays of electrons from higher shells than the L shell are short and throughout the observations made in these experiments electrons occupy the K and L shells only. Hence conversion in the L shell cannot give rise to charge changes of $\Delta q=+2$. Hence the parameters ω_q given in Table I have to be corrected to obtain values of ω_{Kq}, averages of the K-shell fluorescent yields for the electron states which constitute the ensemble in charge state q.

The parameter ω_{Kq} is related to ω_q by

$$\omega_{Kq}=\frac{\lambda_{\mathrm{IC}\,q}}{\lambda_{Kq}}\omega_q \ ,$$

where λ_{Kq} are the probabilities for ions initially in charge state q to decay via K shell IC. The correction to ω_q is small, and only insignificant errors are made if the calculated values of Sec. IV B are used for all $\lambda_{\mathrm{IC}\,q}$ and λ_{Kq}. Applying the corrections gives the values of ω_{Kq} shown in Table I.

Comparisons of data with theory are straightforward for $q=25$, 24 and 23 ions since only one electron state is present. For $q\leq 22$, although a mix of electron states is present, comparisons of decay rates λ_q with theory are essentially unaffected by uncertainties about the mix; comparison of the fluorescent yields ω_{Kq} are more dependent on electron configurations.

B. Electron configurations

1. The $^{57}Fe^{25+}$ charge state

The $2s_{1/2}$ level in the single-electron ion is the only candidate for a lifetime longer than a few ns. The dominant decay mode of this level is by two-photon emission, with a somewhat weaker [17] $M1$ transition. The lifetimes of the $2s_{1/2}$ states in Ar^{17+} and Ni^{27+} have been measured [17,18] to be 3.5 ns and 217 ps, respectively. It may thus be assumed that the observations made in these experiments relate to the electron in the $1s_{1/2}$ state.

2. The $^{57}Fe^{24+}$ charge state

There are seven levels arising from placing both electrons in the $1s$ orbit or one in the $1s$, the other in the L shell. Their descriptions to first order in L-S coupling are

(a) $(1s)^2\,{}^1S_0$,

(b) $1s,2s\,{}^1S_0$,

(c) $1s,2s\,{}^3S_1$,

(d) $1s,2p\ ^1P_1$,

(e) $1s,2p\ ^3P_1$,

(f) $1s,2p\ ^3P_1$,

(g) $1s,2p\ ^3P_2$.

Configuration (b) decays predominantly to the $(1s)^2$ ground state via two-photon emission, and for Ar^{16+} and Ni^{26+} measured lifetimes [17,18] are 2.3 ns and 154 ps, respectively. Hence the lifetime in $^{57}Fe^{24+}$ is less than 2 ns. Configuration (c) decays predominantly via a relativistically induced $M1$ transition to the ground state. For Ar^{16+} and Br^{33+} measured lifetimes [17,19] are 172 ns and 224 ps, respectively. The $M1$ transition rate has been shown [20] to scale as the tenth power of the atomic number Z, and thus the expected lifetime of the $^3S_1$ in $^{57}Fe^{24+}$ is about 4 ns. The code GRASP was used to predict the radiative decay lifetimes of the ^3P and ^1P states. All reach the ground state in a time <3 ns. Hence the observations made in these experiments relate to electrons in the $(1s)^2\ ^1S_0$ ground state.

3. The $^{57}Fe^{23+}$ charge state

There are 15 states arising from configurations in which a hole in the K shell is accompanied by two electrons in L-shell orbits. The $(1s)^1(2s)^1(2p)^1\ ^4P_{5/2}$ level has the longest predicted radiative lifetime of about 5 ns, the remainder having radiative lifetimes shorter than 6×10^{-13} s. The latter time is of the same order as the Auger decay time, and so all ions observed in these experiments with three electrons on, or more, have the K shell fully occupied after a very short time.

The $(1s)^2(2p)^1\ ^2P_{1/2,3/2}$ states have predicted lifetimes for radiative decay to the $(1s)^2(2s)^1\ ^2S_{1/2}$ ground state of ~2 and ~0.3 ns, respectively. Thus our experiments study $^{57}Fe^{23+}$ ions in their ground state, and a vacancy in the K shell produced by IC cannot be filled by Auger emission. This is in agreement with the observed position spectra, which show no second subsidiary peak near the $q=25$ main peak such as would arise from a charge change $\Delta q=+2$ in ions of initial charge $q=23$. The simulations of the data were made using unit value for the parameter ω_{23}.

4. The $^{57}Fe^{22+}$ charge state

There are ten levels which arise from configurations with two electrons in the K shell and two in the L shell, four spin singlets and six spin triplets. Excited singlet states rapidly decay to the $(1s)^2(2s)^2\ ^1S_0$ ground state. Excited triplet states decay to the $(2s)^1(2p)^1\ ^3P_{0,1,2}$ multiplet. The $^3P_1$ state has a predicted lifetime of about 25 ns; the other two multiplet members have long lifetimes. The mix of four-electron states relevant to the experiments is thus hard to determine. For making predictions to compare with the experimental numbers, we assume an initial statistical distribution of L-shell states and estimate that during passage of the spectrograph 40% of the $q=22$ ions are in the $(1s)^2(2s)^2$ configuration and 60% in the $(1s)^2(2s)^1(2p)^1$ configuration. For calculating the ICC's we further assume for $q=22$, 21 and 20 ions that electrons in p orbits are distributed equally between $p_{1/2}$ and $p_{3/2}$ states. This assumption makes only small uncertainties in the predictions.

5. The $^{57}Fe^{21+}$ charge state

There are 15 levels which arise from configurations with three electrons in L-shell orbits accompanying a full K shell; 11 are spin doublets and four spin quadruplets. After a time less than 10^{-10} s, the population is distributed between the $(2s)^2(2p)^1\ ^2P_{1/2,3/2}$ and $(2s)^1(2p)^2\ ^4P_{1/2,3/2,5/2}$ levels. The spin quadruplet levels have predicted half lives of ~40, 100 and 10 ns, in order of increasing angular momentum. The $^2P_{1/2}$ level is the ground state of the ion and the $^2P_{3/2}$ level has a predicted lifetime of $\sim7\times10^{-5}$ s. Again assuming an initial statistical distribution of L-shell electron states, it is estimated that during passage of the spectrograph 70% of the $q=21$ ions are in the configuration $(2s)^2(2p)^1$ and 30% in the configuration $(2s)^1(2p)^2$.

6. The $^{57}Fe^{20+}$ charge state

There are 20 levels which arise from configurations of four electrons in the L shell with the K shell full. The five levels from the $(2p)^4$ configuration decay with lifetimes $<10^{-10}$ s, chiefly to triplet and singlet spin states from the $(2s)^1(2p)^3$ configuration. These, in turn, decay rapidly to $(2s)^2(2p)^2$ states, except for levels with (first-order) description $^5S_2$, $^3P_{1,2}$ and $^1D_2$. It is estimated that during passage of the spectrograph 75% of the $q=20$ ions are in the configuration $(2s)^2(2p)^2$ and 25% in the configuration $(2s)^1(2p)^3$.

7. The $^{57}Fe^{19+}$ charge state

There are 15 levels which arise from configurations of five electrons in the L shell with the K shell full. The three excited spin quadruplet levels decay rapidly to the $(2s)^2(2p)^3\ ^4S_{3/2}$ ground state. Spin doublets from the $(2s)^1(2p)^4$ configuration decay rapidly to spin-doublet states from the $(2s)^2(2p)^3$ configuration. Hence, during passage of the spectrometer, all $q=19$ ions are in the configuration $(2s)^2(2p)^3$.

C. Comparison with theory: λ_q

The total decay probability per unit time, λ_q, of the 14.4-keV level in the ions of charge state q observed in the present experiments is given by

$$\lambda_q=\lambda_\gamma+\lambda_{Kq}+\lambda_{Lq}\ , \tag{10}$$

where λ_γ is the γ-decay rate (assumed constant and equal to the value $7.7\times10^5\ s^{-1}$ obtained from experimental values [8] for the total conversion coefficient and lifetime in the neutral atom), and λ_{Kq} and λ_{Lq} are the K- and L-shell IC rates. Conversion coefficients giving the latter rates were calculated using the standard formalism [21] for $M1$ IC. The bound-state electron wave functions for

the different charge states and electron configurations were calculated using the code GRASP [16]. The continuum electron wave functions used were calculated using the code of Ref. [22]. The penetration term was included and calculated using the surface-current mode [23]. This term is less than 1% of the main term in the present examples. It is sufficient to use $M1$ IC rates for our comparisons, since the intensity of the $E2$ component in the 14.4-keV transition is [8] about 5×10^{-5} and the $E2$ K- and L-shell ICC's are larger than the $M1$ ICC by less than a factor of 50.

Table II gives the predicted α_{Kq} and α_{Lq}. Using the γ-decay rate λ_γ, these ICC's determine the predicted total transition rates given in the penultimate column. The final column shows the experimentally determined λ_q. Figure 4 shows the experimental and predicted values of λ_q. The present experimental results and the predicted λ_q values for the charged ions are consistent at the 70% confidence level. However, using the value of 7.7×10^5 s^{-1} for λ_γ with the calculated total ICC predicts a λ_{total} for the neutral atom nearly two standard deviations from the measured value. If the ICC in the neutral atom were remeasured to be nearer to the predicted value, this would entail a change in the value of λ_γ deduced from the measured lifetime. This, in turn, would reduce the predicted λ_q for the charged ions and worsen the agreement for the present results. This situation calls into question the assumption implicit in Eq. (10) of only three significant decay modes, and also the assumption of constant λ_γ. More theoretical work is needed to clarify the importance of other deexcitation mechanisms [24,25] of the 14.4-keV state, although they are expected to be small. The contribution from the resonant electronic bridge mechanism [25] has been calculated to be less than 0.01%. The nonresonant contribution has so far not been estimated.

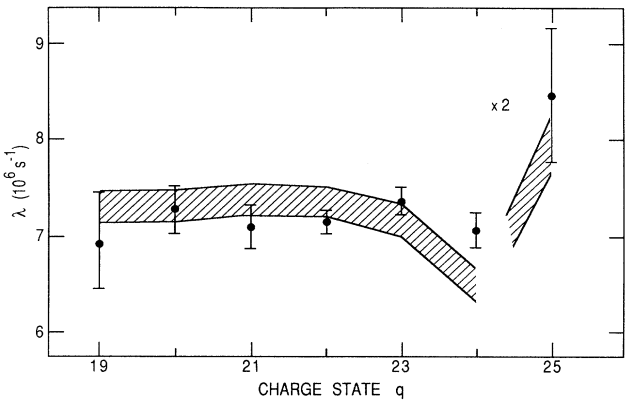

FIG. 4. Experimentally determined values of transition probabilities λ_q using calculated conversion coefficients and experimental γ-ray decay probability. The point for $q=25$ has been plotted ($\times2$) assuming a statistical mix of $q=25$ ions ($\lambda_{25}=3\lambda_{25}(F=1)/8+5\lambda_\gamma/8$). The hatched area represents one standard deviation either side of the predicted λ_q.

Several previous calculations [9,26] have shown that $M1$ ICC's for s orbits are proportional to the appropriate s-electron density at the nucleus to within a few percent. This rough proportionality remains true for highly charged Fe ions, as shown in Table III; however, the precise behavior is less simple. Small changes in the K-electron density consequent upon rearrangement or changing electron numbers do not result in proportional

TABLE II. Comparison of measured and predicted values of the transition probabilities λ_q.

q	Configuration	α_{Kq}	α_{L1q}	α_{L2q}	α_{L3q}	$\alpha_{\text{IC}q}$	λ_q^b (10^6 s^{-1})	λ_q (expt) (10^6 s^{-1})
25	$(1s)^1$: $F=1$	11.20				11.20	9.39(24)	10.0(9)[d]
24	$(1s)^2$	7.41				7.41	6.48(17)	7.06(18)[d]
23	$(1s)^2(2s)^1$	7.86	0.45			8.31	7.17(19)	7.36(14)
22	$(1s)^2(2s)^2$	7.91	0.88			8.79	7.54(20)	
	$(1s)^2(2s)^1(2p)^1$	7.89	0.44	0.010	0.004	8.34	7.19(19)	
							7.33[c](19)	7.16(11)
21	$(1s)^2(2s)^2(2p)^1$	7.82	0.86	0.009	0.004	8.69	7.46(20)	
	$(1s)^2(2s)^1(2p)^2$	7.83	0.43	0.019	0.008	8.29	7.15(19)	
							7.37[c](19)	7.10(23)
20	$(1s)^2(2s)^2(2p)^2$	7.72	0.83	0.019	0.007	8.58	7.38(19)	
	$(1s)^2(2s)^1(2p)^3$	7.69	0.42	0.027	0.011	8.15	7.05(18)	
							7.30[c](19)	7.28(25)
19	$(1s)^2(2s)^2(2p)^3$	7.63	0.81	0.026	0.011	8.48	7.30(19)	6.92(46)
0	Neutral atom	7.68	0.73	0.044	0.018	8.59[a]	7.38(19)	7.06(2)[e]

[a]Includes 0.10 from the $M1$ shell and 0.013 from other shells. Value calculated in Ref. [34] for neutral atom $=8.61$, and in Ref. [9] $=8.58$.

[b]$\lambda_q=\lambda_\gamma(1+\alpha_{\text{IC}q})$ [with $\lambda_\gamma=7.7(2)\times10^5$ s^{-1} as calculated using lifetime and conversion coefficient data [8] for the neutral atom].

[c]From combination of appropriate fractions of the two different configurations.

[d]The values for λ of $6.93(31)\times10^6$ s^{-1} for $q=24$ and $8.80(62)\times10^6$ s^{-1} for the $F=1$ state of the $q=25$ ions reported earlier (Table I of Ref. [7] gives the values for λ_{kq}) are consistent with those obtained from the present work.

[e]Reference [8].

TABLE III. Calculated values of conversion coefficients α_{Kq} and α_{L1q} in the different configurations given, together with calculated values of the 1s and 2s electron densities near the center of the nucleus. The latter are given in atomic units (1 a.u.= 6.75×10^9 electrons/fm^3).

q	Configuration	α_K	ρ_K (10^3 a.u.)	α_K/ρ_K (10^{-3} a.u.$^{-1}$)	α_{L1}	ρ_{L1} (10^3 a.u.)	α_{L1}/ρ_{L1} (10^{-3} a.u.$^{-1}$)
25	$(1s)^1$	4.20[a]	7.48	0.561			
24	$(1s)^2$	7.41	13.97	0.530			
23	$(1s)^2(2s)^1$	7.86[a]	13.58	0.579	0.451	0.790	0.571
22	$(1s)^2(2s)^2$	7.91	13.58	0.582	0.879	1.534	0.573
	$(1s)^2(2s)^1(2p)^1$	7.89	13.55	0.582	0.441	0.771	0.572
21	$(1s)^2(2s)^2(2p)^1$	7.82	13.55	0.577	0.858	1.495	0.574
	$(1s)^2(2s)^1(2p)^2$	7.83	13.53	0.579	0.431	0.751	0.574
20	$(1s)^2(2s)^2(2p)^2$	7.72	13.52	0.571	0.833	1.456	0.572
	$(1s)^2(2s)^1(2p)^3$	7.69	13.51	0.569	0.419	0.731	0.573
19	$(1s)^2(2s)^2(2p)^3$	7.63	13.50	0.565	0.811	1.417	0.572

[a]ICC for ions statistically distributed between $F=1$ and 2 states.

changes to α_K. The present situation is somewhat different from those discussed previously, in that as the charge state changes, all physical parameters which determine the K-conversion coefficient change; the K-electron binding energy, the kinetic energy of the continuum electron, and the atomic potential used to calculate the continuum electrons wave function. The energy of the nuclear transition is also low and comparable to the K-shell binding energies. All these factors have a critical influence on the calculated K-shell coefficients.

The s-electron density at the nucleus is influenced to a small extent by several effects additional to those due to changing electron numbers and configurations. Two such arise from the nuclear charge-distribution and from high-order quantum electrodynamic (QED) corrections. The predictions given in Tables II and III were calculated using a spherical nuclear charge distribution given by a two-parameter Fermi function [16] with a radius $R_{1/2}$ of 4.19 fm and a skin thickness of 0.523 fm. These parameter are acceptably close to the values determined for the ground states of ^{56}Fe and ^{58}Fe nuclei from electron-scattering experiments [27]. The sensitivity of the predicted coefficients α_T to $R_{1/2}$ was obtained from calculations to be $\sim0.3\%$ per Fermi for the neutral atom and $\sim1.5\%$ per Fermi for the single-electron ion.

The influence of higher-order QED effects are not known. They have been estimated [29] to change the binding energy of H-like U ions by less than one part in 10^4 and so are expected to be small. Nuclear charge distributions and QED effects can in principle be studied with accurate measurements of $M1$ ICC's in highly charged ions. Measurements of sufficient accuracy may be possible in suitable cases with the technique described in this paper or with charge-changing experiments on heavy ion beams in storage rings.

D. Comparison with theory: ω_{Kq}

The K-shell fluorescent yield of an atomic state which contains a hole in the K shell is the ratio of the probability per unit time for decay via K x-ray emission to the total decay probability per unit time. The ions observed in the present experiments in charge state q (for $q\leq22$) are in a mixture of electronic states, and hence they are also in a mix of states after IC decays have produced K vacancies. As discussed in Sec. IV A, there is some uncertainty about this mix. The ω_{Kq} measured in the experiments are averages of the fluorescent yields over the electron states in the charge state $(q+1)$ weighted according to their fraction of the population. Because of the uncertainty in these fractions we have not attempted to calculate ω_{Kq}. Instead, we adopt approximate procedures and make estimates to compare with the observed trend. This trend is for ω_{Kq} to decrease as q decreases, and for ω_{Kq} to be higher than the measured [29] value of 0.34(1) in the neutral atom.

The effect on Auger transition rates of incomplete electron shells has been treated [30] in the approximation that electron wave functions in ionized atoms are the same as in the neutral atoms. For an atom with one hole in the K shell, n holes in the 2s subshell and p holes in the 2p subshell, the KL_1L_{23} and $KL_{23}L_{23}$ Auger transition rates are given by

$$W_{1np}(KL_1L_{23})=(2-n)(6-p)W_{100}(KL_1L_{23})/12\ , \quad (11)$$

$$W_{1np}(KL_{23}L_{23})=(6-p)(5-p)W_{100}(KL_{23}L_{23})/30\ , \quad (12)$$

where W_{100} are the neutral atom rates [30]. For two electrons in the L_1 subshell the rate $W_{10p}(KL_1L_1)$ is unchanged from the neutral atom rate.

The formulas for W_{1np} refer to rates summed and averaged over all states arising from the incomplete-shell configurations, and so are not strictly applicable to the mixes of states observed in these experiments. Nevertheless, we use these formulas in an approximate procedure similar to that of Ref. [31] to estimate the K-shell fluorescent yields in the different electron configurations. If λ_{x0} is the radiative transition probability per unit time for filling a K hole from a full L shell, following Ref. [31] we use $\lambda_{xp}=(6-p)\lambda_{x0}/6$ as the rate from an L shell with p holes in L_{23} orbits. For the configuration $(1s)^1(2s)^2$ the

x-ray emission rate can be unambiguously calculated, and in that particular instance the calculated rate was used. For the total Auger transition rate we use

$$W^T_{1np} = W_{100}(KL_1L_1) + W_{1np}(KL_1L_{23}) + W_{1np}(KL_{23}L_{23}) , \quad (13)$$

which gives, finally,

$$\omega_{1np} = \frac{\lambda_{xp}}{W^T_{1np} + \lambda_{xp}} . \quad (14)$$

The first term on the right-hand side of Eq. (13) is nonzero only if n equals zero, and the third term is nonzero only if two or more electrons occupy $2p$ orbits. The rates W_{100} were obtained from Ref. [32] and the rate λ_{x0} was calculated to be 6×10^{14} s^{-1}.

For charge state $q=22$ before IC, 40% of the ions are in the $(1s)^2(2s)^2$ configuration. After IC they are assumed to be all in the $(1s)^1(2s)^2\,^2S_{1/2}$ state, which has an Auger decay rate of 7.8×10^{13} s^{-1} and an x-ray decay rate of 2×10^{13} s^{-1}. Hence, for this 40% of the ions, the fluorescent yield is 0.21. For 60% of ions in the $(1s)^2(2s)^1(2p)^1$ configuration before IC, there are several possible electron states after IC, and we use the procedure described above to estimate the fluorescent yield to be 0.83. Combining the results for the two sets of ions gives $\omega_{K22}=0.58$, compared with the fitted value of 0.62(1).

For charge state $q=21$, after IC 30% of ions are in the $(1s)^1(2s)^1(2p)^2$ configuration and are estimated to have a fluorescent yield of 0.71; 70% are in the $(1s)^1(2s)^2(2p)^1$ configuration and are estimated to have a fluorescent yield of 0.45. Combination gives $\omega_{K21}=0.53$, compared with the measured value of 0.50(1). For charge state $q=20$, after IC, 75% of ions are in the $(1s)^1(2s)^2(2p)^2$ configuration and are estimated to have a fluorescent yield of 0.50; 25% are in the $(1s)^1(2s)^1(2p)^3$ configuration and are estimated to have a fluorescent yield of 0.63. Combination gives $\omega_{K20}=0.53$, compared with the measured value of 0.48(2). For charge state $q=19$, after IC all ions are in the configuration $(1s)^1(2s)^2(2p)^3$ and are estimated to have a fluorescent yield of 0.48, compared with the measured value of 0.50(6). Figure 5 shows experimental and estimated values of ω_K as a function of charge q on ions before K-vacancy production.

It is interesting to use the approximate procedure to estimate ω_{K16} for ions initially in the configuration $(1s)^2(2s)^2(2p)^6$. The estimated fluorescent yield is 0.38, compared with the neutral atom value of 0.34(1). It is clear that the scaling procedures adopted describe the trend observed in ω_{Kq} values as electrons are added. However, as noted before [33], the approximation must be used with caution and more rigorous calculations made for prescribed mixtures of electron states.

V. SUMMARY

A technique has been developed for measuring atomic and nuclear properties of highly ionized atoms. It has been applied to the measurement of decay rates of a nuclear isomer in ^{57}Fe ions of different states of ionization. The decay rates of the isomer in different electronic configurations determine the K-shell internal-conversion coefficients, which are sensitive to details of the electron wave functions. The measured ICC's have been compared to predictions made using electron wave functions obtained from relativistic mean-field calculations. Good agreement was found between theory and experiment. K-shell fluorescent yields in ^{57}Fe ions of different charge states have also been measured. These yields are averages over the long-lived electron states present in the observed beams. Predicted estimates of the behavior of the fluorescent yields with ion charge state show the same trend as the measurements. Accurate experiments of the general type described here offer probes for the several effects which influence inner-shell electron wave functions in the vicinity of the nucleus, and provide opportunities to study long-lived electron states in ionic beams.

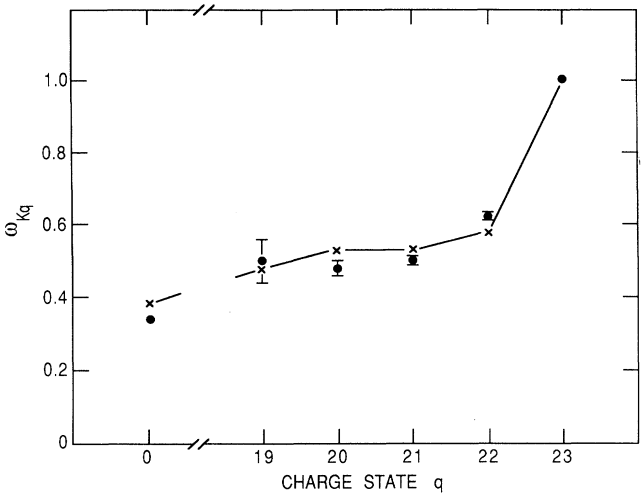

FIG. 5. Experimentally determined values of K-shell fluorescent yields ω_{Kq} (closed circles) compared to values estimated from the model described in Sec. IV C (crosses). The model estimate of ω_{Kq} for $q=16$ is plotted for convenience above the experimental value for the neutral atom.

ACKNOWLEDGMENTS

We wish to thank F. Parpia and I. P. Grant for providing us with a copy of the code GRASP. We thank A. R. Barnett and P. Ottewell for the installation of that code on SUN workstations, and R. W. Dunford, S. Koonin, M. Paul, J. Weneser, and Xiangdon Ji for other help and discussions. This work was supported in part by NATO Grant No. 0210-87, by grants from the U.S. Department of Energy, Nuclear Physics Division under Contract No. W-31-109-ENG-38, and by the Science and Engineering Research Council of the United Kingdom.

[1] U. Feldman, Phys. Scripta **24**, 681 (1981).
[2] B. C. Fawcett, Z. Phys. D **21**, 51 (1991).
[3] K. W. Hill, S. von Goeler, M. Bitter, L. Campbell, R. D. Cowan, B. Fraenkel, A. Greenberger, R. Horton, J. Hovey, W. Roney, N. R. Southoff, and W. Stodiek, Phys. Rev. A **19**, 1770 (1979).
[4] J. Dubau and S. Volonte, Rep. Prog. Phys. **43**, 199 (1980).
[5] W. R. Johnson and K. T. Cheng, in *Atomic Inner Shell Physics,* edited by B. Craseman (Plenum, New York, 1985).
[6] W. R. Phillips, K. E. Rehm, W. Henning, I. Ahmad, J. P. Schiffer, B. G. Glagola, and T. F. Wang, J. Phys. (Paris) Colloq. **48**, C9-311 (1987).
[7] W. R. Phillips, I. Ahmad, D. W. Banes, B. G. Glagola, W. Henning, W. Kutschera, K. E. Rehm, J. P. Schiffer, and T. F. Wang, Phys. Rev. Lett. **62**, 1025 (1989).
[8] T. W. Burrows and M. R. Bhat, Nucl. Data Sheets **47**, 1 (1986).
[9] P. Rüegsegger and W. Kündig, Helv. Phys. Acta **46**, 165 (1973).
[10] M. Ulrickson, R. Hensler, D. Gordon, N. Benczer-Koller, and H. DeWaard, Phys. Rev. C **9**, 326 (1974).
[11] A. Krasznahorkay, T. Kibedi, and Z. S. Dombradi, Z. Phys. A **323**, 125 (1986).
[12] J. E. Spencer and H. A. Enge, Nucl. Instrum. Methods **49**, 181 (1967).
[13] K. E. Rehm and F. L. H. Wolfs, Nucl. Instrum. Methods, Phys. Res. Sect. A **273**, 262 (1988).
[14] S. Kowalski and H. A. Enge, MIT 1986 version of RAY-TRACE, unpublished.
[15] E. L. Church and J. Weneser, Ann. Rev. Nucl. Sci. **10**, 193 (1960).
[16] K. G. Dyall, I. P. Grant, C. T. Johnson, F. A. Parpia, and E. P. Plummer, Comput. Phys. Commun. **55**, 425 (1989).
[17] R. Marrus and R. W. Schmeider, Phys. Rev. A **5**, 1160 (1972).
[18] R. W. Dunford, M. Hass, E. Bakke, H. G. Berry, C. J. Liu, and M. L.A. Raphaelian, Phys. Rev. Lett. **62**, 2809 (1989).
[19] R. W. Dunford, D. A. Church, C. J. Liu, H. G. Berry, M. L. A. Raphaelian, M. Hass, and J. L. Curtis, Phys. Rev. A **41**, 4109 (1990).
[20] G. Feinberg and J. Sucher, Phys. Rev. Lett. **26**, 681 (1971).
[21] H. C. Pauli, K. Alder and R. M. Steffen, in *Electromagnetic Interaction in Nuclear Spectroscopy,* edited by W. D. Hamilton (North-Holland, Amsterdam, 1975).
[22] R. Der, D. Hinnerburg, and M. Nagel, Comput. Phys. Commun. **18**, 401 (1979).
[23] M. A. Listengarten and I. M. Band, Izv. Akad. Nauk SSSR, Ser. Fiz. **38**, 1588 (1974).
[24] D. Kekez, A. Ljubicic, K. Pisk, and B. Logan, Phys. Rev. Lett. **55**, 1366 (1985).
[25] V. M. Kolomietz and V. N. Kondratjev, Z. Phys. A **335**, 379 (1990).
[26] I. M. Band, L. A. Sliv, and M. B. Trzhaskovskaja, Nucl. Phys. A **156**, 170 (1970).
[27] H. De Vries, C. W. De Jager, and C. De Vries, At. Data Nucl. Data Tables **36**, 495 (1987).
[28] G. Soff and P. J. Mohr, Phys. Rev. A **40**, 2127 (1989).
[29] W. Bambynek, B. Craseman, R. W. Fink, H. U. Freund, H. Mark, C. D. Swift, R. E. Price, and P. Venugopala Rao, Rev. Mod. Phys. **44**, 716 (1972).
[30] E. J. McGuire, in *Atomic Inner Shell Processes* (Ref. [5]).
[31] F. P. Larkins, J. Phys. B **4**, L29 (1971).
[32] M. H. Chen, B. Crasemann, and H. Mark, At. Data Nucl. Data Tables **24**, (1979).
[33] C. P. Bhalla and M. Hein, Phys. Rev. Lett. **30**, 39 (1973).
[34] K. Alder, U. Raff, and G. Bauer, Helv. Phys. Acta **45**, 771 (1972).